Supporting Information

1. Pathogen dynamics

Here we describe the probabilistic calculus for the evolution of a quantitative trait and the concurrent population dynamics in a given ecological niche, and we derive the minimum-leverage relations used in the main text.

Stochastic evolution of pathogen traits. These dynamical processes of a quantitative trait G and of the population size N are generically coupled by selection: fitness effects generated by the evolution of the trait change the population's carrying capacity, which, in turn, affects the natural variation of the trait and the speed of evolution. In the main text, we use the diffusion equation (17) to describe the evolution of the population mean trait,

$$\Gamma(t) = \int G\,\rho(G,t)\,dG; \tag{S1}$$

here $\rho(G,t)$ is the trait distribution in the evolving population, which is generated by common mutations with individually small effects. The diffusive evolution of Γ depends on diffusion and on response coefficients [1, 2]. The trait diffusion coefficient D is given by the increase of the heritable trait variance per generation by new mutations,

$$D = U\epsilon_0^2, \tag{S2}$$

which depends on the total mutation rate at trait-encoding genomic sites, U, and the mean square trait effect of these mutations, ϵ_0^2. The trait response to the entropic force $(dS(\Gamma)/d\Gamma)$ equals D, which ensures the neutral trait dynamics leads to the correct equilibrium trait distribution given by Eq. (S6) below. The trait response to selection depends on the response coefficient

$$\Delta = 2DN_e, \tag{S3}$$

which equals the equilibrium expectation value of the heritable trait variance. Over a broad range of evolutionary conditions, Eq. (S3) can be regarded as a defining relation for the effective population size N_e [2], similar to the relation $\pi = 2\mu N_e$ that links the sequence variance at neutral sites to the point mutation rate μ [3]. The effective population size N_e given by Eq. (S3) is also broadly related to the coalescence time, $\tau_c = 2N_e$ [4, 5]. The relation of N_e to the census population size N depends on the system and its evolutionary mode; some relevant cases are listed below.

Pathogen population dynamics. The population size dynamics of Eq. (18) can be derived from a simple birth-death model. We consider a Poisson process with birth rate $b(G,N)$ and death rate $d(G,N)$, in which the reproductive rate

$$r(G,N) \equiv b(G,N) - d(G,N) = f_p(\Gamma) - cN \ll 1 \tag{S4}$$

depends on the population size and the niche constraint parameter c, and the constraint $b(G,N) + d(G,N) = 1$ is satisfied. This model generates the deterministic population dynamics

$$\dot{N} = \bar{r}(\Gamma,N)N = \bar{f}_p(\Gamma)N - cN^2, \tag{S5}$$

www.pnas.org/cgi/doi/10.1073/pnas.1920263117

where overbars denote averages with respect to the trait distribution $\rho(G,t)$. To leading order in r, the birth-death model generates the processes $1 \to 0$ with probability $p = 1/4$, $1 \to 1$ with $p = 1/2$, $1 \to 2$ with $p = 1/4$, leading to population size fluctuations with a diffusion constant $N/2$, cf main text. Together, we obtain the population dynamics given in Eq. (17); we use the approximation $\bar{f}(\Gamma) \approx f(\Gamma)$ explained below. Other models of this class differ in their detailed birth and death rates but generate a similar diffusive dynamics of large population sizes (i.e., in a Taylor expansion about $\bar{N}$) [6, 7].

Neutral eco-evolutionary equilibrium. In the special case of neutral evolution, i.e., for a trait- and time-independent absolute fitness $f_p(G,t) = f_0$, the evolutionary dynamics given by Eq. (17) has an equilibrium distribution

$$Q_0(\Gamma) = \frac{1}{Z_{\Gamma,0}} \exp[S(\Gamma)]. \tag{S6}$$

According to this distribution, the probability of a given Γ value is proportional to the density of sequence states mapped onto that value. Here we assume equiprobability of sequence states under neutral evolution; i.e., we ignore sequence composition biases at trait loci, which are usually small and irrelevant for this paper.

Similarly, the population dynamics given by Eq. (18) has an equilibrium distribution

$$Q_0(N) = \frac{1}{Z_{N,0}} \exp\left[-c\,(N - \bar{N}_0)^2\right], \tag{S7}$$

which describes stable fluctuations of the population size around the carrying capacity of the ecological niche,

$$\bar{N}_0 = \frac{f_0}{c}. \tag{S8}$$

Here we assume that this carrying capacity is large enough so that the probability of fluctuations leading to extinction of the population can be neglected [8].

Evolutionary stationary states under selection. The evolution of the mean population trait Γ, as described by Eq. (17), responds to the mean population fitness

$$\bar{f}_p(t) = \int \rho(G,t)\, f_p(G,t)\, dG. \tag{S9}$$

Given a trait distribution of approximate Gaussian form, we can write

$$\bar{f}_p = f_p(\Gamma) + \frac{1}{2}\Delta f_p''(\Gamma) + \ldots; \tag{S10}$$

for sufficiently smooth fitness functions, this leads to the approximation $\bar{f}_p(\Gamma) \approx f_p(\Gamma)$ used in the main text and below.

In any time-independent fitness landscape $f_p(\Gamma)$, the dynamics of Eq. (17) generates an equilibrium distribution

$$Q_{\rm eq}(\Gamma) = \frac{1}{Z_\Gamma} \exp[\psi_p(\Gamma)] \tag{S11}$$

given in terms of the *free fitness*

$$\psi_p(\Gamma) = S(\Gamma) + \mathcal{F}(\Gamma), \tag{S12}$$

which is the sum of the entropy $S(\Gamma)$ defined in Eq. (S6) and the fitness potential

$$\mathcal{F}(\Gamma) = \int_{\Gamma_0}^{\Gamma} 2N_e(\Gamma)\, \bar{f}_p'(\Gamma)\, d\Gamma. \tag{S13}$$

The integral on the r.h.s. contains an arbitrary reference point Γ_0, variations of which can be absorbed into the normalization factor Z_Γ. The derivative of the free fitness with respect to Γ defines the evolutionary force

$$\partial_\Gamma \psi_p(\Gamma, \zeta) = 2N_e(\Gamma)\, \bar{f}_p'(\Gamma, \zeta) + S_p'(\Gamma). \tag{S14}$$

as given in Eq. (1) of the main text.

The fitness potential (S13) takes into account that the effective population size generically depends on the trait value, $N_e = N_e(\Gamma)$. Such variation is often relevant in pathogen systems, where census population sizes can vary considerably during an evolutionary process. Variable effective population sizes generate an inhomogeneous response to selection. The form of this response depends on the evolutionary mode of the system and on the underlying ecology, which can have a complex impact on one another. We can distinguish two broad regimes where simplifications lead to tractable computations. (i) If the coalescence process is dominated by genetic drift, the coalescence time exceeds the relaxation time of the population size in a stable population, $\tau_c \gg \tau_N$, as shown in the next paragraph. In this case, we use the approximation

$$N_e(\Gamma) \approx \bar{N}(\Gamma); \tag{S15}$$

hence, the evolutionary dynamic decouples from the instantaneous census population size and becomes autonomous. If the evolutionary range of Γ generates only small relative differences in absolute fitness, $\delta f/f = \delta\bar{N}/\bar{N} \ll 1$, we can further approximate N_e by a constant. The fitness potential then reduces to the standard form of a reduced fitness,

$$\mathcal{F}(\Gamma) = 2N_e f_p(\Gamma). \tag{S16}$$

(ii) Under clonal evolution in large asexual populations, the coalescence process is dominated by interference effects, which generates effective population sizes with a very weak dependence on N. Here we use the approximation

$$N_e \sim (\log N)^{1/3}, \tag{S17}$$

which can be derived from a travelling fitness wave model [5]. The dominant contribution to the integral in equation (S13) then comes from variations in $f_p(\Gamma)$; hence, for the leading-order estimates used below, we can still use the approximation (S16).

Importantly, given strongly varying pathogen population sizes, the mode of pathogen evolution and the scaling of N_e are themselves subject to control and can change in the course of a control processs. For example, the breeding phase protocol for adaptive trait formation described in the main text has a crossover from a drift regime to a clonal interference regime as a function of the pathogen population size. The corresponding effective population sizes, Eq. (S15) and (S17), enter the scaling of the control score $J_{\rm br}(G)$ in Eq. (31). For extreme non-equilibrium processes, which involve likely trajectories with population sizes far from the carrying capacity, we expect the evolutionary process to couple to the path-dependent census population size. The fluctuation statistics of this regime is more involved and falls outside the scope of this paper.

Ecological states under selection. The population dynamics of Eq. (18) reaches a simple conditional equilibrium distribution

$$Q_{\rm eq}(N|\Gamma) = \frac{1}{Z_N}\,\exp\left[-c\,(N-\bar{N}(\Gamma))^2\right] \tag{S18}$$

with the trait-dependent carrying capacity

$$\bar{N}(\Gamma) = \frac{f_p(\Gamma)}{c}, \tag{S19}$$

if the relaxation time of the population size, τ_N, is much smaller than the coalescence time, $\tau_c = 2N_e$. This condition is self-consistently fulfilled for stable populations with coalescence dominated by genetic drift. To show this, we estimate the coalescence time in terms of the time-averaged census population size at a given trait value, $\tau_c \sim 2\bar{N} - O(\bar{N}^{1/2})$. The relaxation time $\tau_N = 1/(c\bar{N})$ follows directly from Eq. (18). Together, the condition for time separation between population dynamics and evolution reads

$$\frac{\tau_N(\Gamma)}{\tau_c(\Gamma)} \sim \frac{1}{2c\bar{N}^2(\Gamma)} = \frac{\langle (N-\bar{N}(\Gamma)^2)\rangle}{\bar{N}^2(\Gamma)} \ll 1. \tag{S20}$$

This relation involves the variance of the population size scaled by the squared carrying capacity, which is small for stable populations far from stochastic extinctions. If the evolutionary process is also at equilibrium, we can then combine the distributions (S11) and (S18) into an equilibrium distribution of the joint eco-evolutionary dynamics,

$$Q_{\rm eq}(\Gamma, N) = Q_{\rm eq}(\Gamma)\,Q_{\rm eq}(N|\Gamma) = \frac{1}{Z}\,\exp\left[\mathcal{F}(\Gamma) - c\,(N-\bar{N}_0)^2\right]. \tag{S21}$$

On the other hand, clonal evolution under strong interference selection generates shorter coalescence times τ_c, which can become comparable to τ_s. In that case, the stationary distribution $Q(\Gamma, N)$ no longer has the simple equilibrium form (S21); it becomes a non-equilibrium state with a nonvanishing probability current. However, the marginal trait distribution retains the equilibrium form $Q_{\rm eq}(\Gamma)$ given by Eq. (S11), as long as the trait dynamics remains (approximately) autonomous.

Non-equilibrium fluctuation theory and evolutionary flux. The stochastic dynamics given by Eqs. (17) can be applied to estimate the probability of adaptive eco-evolutionary processes in a generically time-dependent fitness seascape $f_p(\Gamma, t)$. A realization of the evolutionary process in a given population maps an evolutionary path $\mathbf{\Gamma}$, which is defined by a continuous function $\Gamma(t)$ connecting an initial population state with mean trait Γ_0 at time t_0 to a final state with mean trait Γ_f at time t_f ($t_0 \le t \le t_f$). The relevant non-equilibrium fluctuation theory is contained in refs. [9, 10, 11, 12] and reviewed in ref. [13]; the evolutionary fluctuation theory used here has been established in ref. [14]. Here we develop the probabilistic calculus for pathogen trait paths $\mathbf{\Gamma}$; in the following section, we generalize this calculus to control processes with paths $(\mathbf{\Gamma}, \boldsymbol{\zeta})$.

The probability (density) $\mathcal{P}(\mathbf{\Gamma})$ of the trait path $\mathbf{\Gamma}$ evolving in the free fitness seascape $\psi_p(\Gamma, t)$ is the product of the probability of the initial state at the time t_0 and the conditional probability (or propagator) of the subsequent path for given initial state,

$$\mathcal{P}(\mathbf{\Gamma}) = Q(\Gamma_0, t_0)\,G(\mathbf{\Gamma}). \tag{S22}$$

This forward path probability is to be compared with the probability

$$\mathcal{P}^T(\mathbf{\Gamma}^T) = Q(\Gamma_f, t_f)\, G^T(\mathbf{\Gamma}^T) \tag{S23}$$

of the time-reversed (backward) path $\mathbf{\Gamma}^T$, which is defined by the map

$$\Gamma^T(t) \equiv \Gamma(t_f + t_0 - t) \qquad (t_0 \le t \le t_f) \tag{S24}$$

evolving in the time-reversed free fitness seascape

$$\psi_p^T(\Gamma, t) \equiv f_p(\Gamma, t_f + t_0 - t) \qquad (t_0 \le t \le t_f). \tag{S25}$$

A key result of non-equilibrium fluctuation theory is the time-reversal relation

$$\frac{G(\mathbf{\Gamma})}{G^T(\mathbf{\Gamma}^t)} = \exp[\Theta_p(\mathbf{\Gamma})], \tag{S26}$$

which relates the conditional probabilities (propagators) of the forward and the backward path, as defined in Eqs. (S22) and (S23). Here $\Theta_p(\mathbf{\Gamma})$ is the evolutionary flux of the forward path,

$$\Theta_p(\mathbf{\Gamma}) = \int_{t_0}^{t_f} \frac{\partial}{\partial \Gamma} \psi_p(\Gamma(t), t)\, \dot{\Gamma}(t)\, dt = \Theta_0(\mathbf{\Gamma}) + \Xi(\mathbf{\Gamma}), \tag{S27}$$

where

$$\Theta_0(\mathbf{\Gamma}) = S(\Gamma_f) - S(\Gamma_0) \tag{S28}$$

is the neutral flux and

$$\Xi(\mathbf{\Gamma}) = \int_{t_0}^{t_f} 2N_e(\Gamma(t))\, \frac{\partial}{\partial \Gamma} f_p(\Gamma(t), t)\, \dot{\Gamma}(t)\, dt \tag{S29}$$

is the scaled fitness flux of the forward path $\mathbf{\Gamma}$. The definition of the evolutionary flux, Eq. (S27), and the time-reversal relation, Eq. (S26), apply to evolutionary dynamics by common mutations and by discrete, large-effect mutations. For a discrete substitution process changing an initial trait G_1 to a derived trait G_2, the population mean trait and mean free fitness can be written in terms of the frequency of the derived allele,

$$\Gamma = x\, G_2 + (1 - x)\, G_1, \tag{S30}$$

$$\bar{\psi}_p(t) = x\, \psi_p(G_2, t) + (1 - x)\, \psi_p(G_1, t), \tag{S31}$$

and the evolutionary flux takes the form [14]

$$\Theta_p(\mathbf{\Gamma}) = \int_{t_0}^{t_f} \frac{\partial}{\partial x} \psi_p(x(t), t)\, \dot{x}(t)\, dt. \tag{S32}$$

The relations (S26) – (S29) can be derived by a straightforward generalization of the analogous result in ref. [14]. They are valid as long as the evolutionary dynamics can be written in an (approximately) autonomous form, i.e., with an effective population size $N_e(\Gamma)$. As discussed above, this includes evolutionary parameter regimes with coalescence dominated by genetic drift or by interference selection.

In the special case of evolutionary equilibrium in a time-independent fitness landscape, the evolutionary flux $\Theta_p(\mathbf{\Gamma})$ reduces to the difference in free fitness between the final and initial state of the path $\mathbf{\Gamma}$,

$$\Theta_p(\mathbf{\Gamma}) = \log \frac{Q_{\rm eq}(\Gamma_f)}{Q_{\rm eq}(\Gamma_0)} = \psi_p(\Gamma_f) - \psi_p(\Gamma_0). \tag{S33}$$

This result follows by comparison of Eqs. (S28), (S29) with Eq. (S11) and expresses detailed balance of the evolutionary equilibrium state; i.e.,

$$\frac{\mathcal{P}_{\rm eq}(\mathbf{\Gamma})}{\mathcal{P}_{\rm eq}(\mathbf{\Gamma}^T)} = \frac{Q_{\rm eq}(\Gamma_0)}{Q_{\rm eq}(\Gamma_f)} \exp[\Theta_p(\mathbf{\Gamma})] = 1. \tag{S34}$$

In the regime of fast population dynamics ($\tau_N \ll \tau_c$), this probabilistic calculus can be generalized to the full eco-evolutionary dynamics, which is described by joint paths $(\mathbf{\Gamma}, \mathbf{N})$ of pathogen trait and population size. The time-reversal relation for the joint process takes the form

$$\frac{G(\mathbf{\Gamma}, \mathbf{N})}{G^T(\mathbf{\Gamma}^t, \mathbf{N}^T)} = \exp\left[\Theta_p(\mathbf{\Gamma}) + \tilde{\Theta}_p(\mathbf{\Gamma}, \mathbf{N})\right] \tag{S35}$$

with the population size flux

$$\tilde{\Theta}_p(\mathbf{\Gamma}, \mathbf{N}) = -\frac{c}{2}\left[(N_f - \bar{N}(\Gamma_f))^2 - (N_i - \bar{N}(\Gamma_0))^2\right]. \tag{S36}$$

Fitness flux theorem. An immediate consequence of the time-reversal relation (S26) is the identity

$$\left\langle \exp(\Theta_p + \Delta\Sigma_p)\right\rangle_{t_0,t_f} = 1. \tag{S37}$$

Here $\langle \dots \rangle_{t_0,t_f}$ denotes averages over the ensemble of paths $\mathbf{\Gamma}$ in the time interval (t_0, t_f), $\Theta_p(\mathbf{\Gamma})$ is the evolutionary flux of a given path $\mathbf{\Gamma}$ defined by Eqs. (S26) – (S29), and $\Delta\Sigma_p(\mathbf{\Gamma}) \equiv \Sigma_p(\Gamma_f, t_f) - \Sigma_p(\Gamma_0, t_0)$, where

$$\Sigma_p(\Gamma, t) = -\log Q(\Gamma, t) \tag{S38}$$

is the local entropy of the trait value Γ. We note that this local entropy is defined from the trait distribution $Q(\Gamma, t)$ and is complementary to the entropy $S(\Gamma)$, which counts sequence states at a given trait value and appears in Eqs. (S6) and (S12).

Following standard fluctuation theory, the identity (S37) is proved by using Eqs. (S22) and (S26) to rewrite the path weight, $\mathcal{P}(\mathbf{\Gamma}) \exp[\Theta_p(\mathbf{\Gamma}) + \Delta\Sigma_p(\mathbf{\Gamma})] = \mathcal{P}^T(\mathbf{\Gamma}^T)$, and integrating over the path ensemble; Eq. (S37) then reduces to the normalization condition $\int_{\mathbf{\Gamma}^T} \mathcal{P}^T(\mathbf{\Gamma}^T) = 1$. By defining the difference in local relative distance to the neutral ensemble between the final and the initial state of the path $\mathbf{\Gamma}$,

$$\Delta\mathcal{H}(\mathbf{\Gamma}) = \log \frac{Q(\Gamma_f, t_f)}{Q_0(\Gamma_f)} - \log \frac{Q(\Gamma_0, t_0)}{Q_0(\Gamma_0)}, \tag{S39}$$

we can rewrite Eq. (S37) in an equivalent form containing the scaled fitness flux,

$$\left\langle \exp(\Xi - \Delta\mathcal{H})\right\rangle_{t_0,t_f} = 1, \tag{S40}$$

Details of definitions and derivations are given in ref. [14]. The flux identities (S37) and (S40) are valid for any evolutionary process given by stochastic equations of the form (17). Importantly, they do not depend on specific properties of the initial and the final state; that is, they are valid over any subperiod $(t_1, t_2) \subset (t_0, t_f)$.

By applying Jensen's inequality to Eq. (S37), we obtain the inequality

$$\big\langle \Theta_p \big\rangle_{t_0,t_f} + \big\langle \Delta\Sigma_p \big\rangle_{t_0,t_f} \geq 0, \tag{S41}$$

which is again valid for any subperiod $(t_1, t_2) \subset (t_0, t_f)$. Here and in the following relations, equality applies to equilibrium and strict inequality to spontaneous processes (i.e., non-equilibrium processes that take place with a finite speed). In the special case of a time-independent fitness landscape, this relation can be rewritten in terms of free fitness differences,

$$\langle \psi_p(t_f) \rangle - \langle \psi_p(t_0) \rangle \geq -\big\langle \Delta\Sigma_p \big\rangle_{t_0,t_f}. \tag{S42}$$

In the main text, we use the deterministic form of the inequality (S41),

$$\Theta_p(\mathbf{\Gamma}) \geq 0; \tag{S43}$$

see Eq. (3). This form emerges in two ways: (i) For traits with a sufficiently large number of encoding genome sites, the distributions $\Sigma_p(\Gamma, t_0)$ and $\Sigma_p(\Gamma, t_f)$ become peaked around the maximum-likelihood values Γ_i^* and Γ_f^*, respectively. Integrating over these distributions, neglecting the subleading contribution from the $\Delta\Sigma_p$ term, and dropping the star notation leads to the form (S43), in analogy with the thermodynamic limit. In practice, the form (S43) provides already a reasonable approximation for transcriptional protein-protein binding traits that are encoded in $\sim 10 - 20$ sequence sites. (ii) A similar dominance of the Θ_p term in equation (S41) arises in the regime of large N_e, which corresponds to large scaled selection amplitudes $\mathcal{F}(\Gamma)$. The relation (S43) says the trait moves on average uphill on the instantaneous free fitness landscape $\psi_p(\Gamma, t)$, which is the sum of the time-dependent fitness potential $\mathcal{F}(\Gamma, t)$ and the Boltzmann entropy $S(\Gamma)$, defined as the log number of sequence states with trait value Γ.

In the special case of evolutionary equilibrium in a time-independent (or slowly varying) fitness landscape, the relation (S43) reduces to the inequality (5),

$$\psi_p(\Gamma_f) - \psi_p(\Gamma_0) \equiv [\mathcal{F}(\Gamma_f) - \mathcal{F}(\Gamma_0)] + [S(\Gamma_f) - S(\Gamma_0)] \geq 0. \tag{S44}$$

2. Control dynamics

Fluctuation theory of instantaneous-update control. The fluctuation relations derived in the previous section generalize to eco-evolutionary control processes with instantaneous update, which are described by control paths $(\mathbf{\Gamma}, \boldsymbol{\zeta})$. Such processes include pathogen evolution by common and by discrete, large-effect mutations, as well as control dynamics by local and greedy update rules. For a control process governed by free fitness and payoff landscapes $\psi_p(\Gamma, \zeta)$, $\psi_h(\Gamma, \zeta)$, the evolutionary flux of the pathogen, Eq. (S27), takes the form

$$\Theta_p(\mathbf{\Gamma}, \boldsymbol{\zeta}) = \int_{t_0}^{t_f} \partial_\Gamma \, \psi_p(\Gamma(t), \zeta(t)) \, \dot{\Gamma}(t) \, dt. \tag{S45}$$

In a similar way, we define the host flux

$$\Theta_h(\mathbf{\Gamma}, \boldsymbol{\zeta}) = \int_{t_0}^{t_f} \partial_\zeta \, \psi_h(\Gamma(t), \zeta(t)) \, \dot{\zeta}(t) \, dt. \tag{S46}$$

The joint process of pathogen evolution and control has a time reversal relation analogous to Eq. (S26),

$$\frac{G(\mathbf{\Gamma}, \boldsymbol{\zeta})}{G(\mathbf{\Gamma}^T, \boldsymbol{\zeta}^T)} \quad = \quad \exp[\Theta_p(\mathbf{\Gamma}, \boldsymbol{\zeta}) + \Theta_h(\mathbf{\Gamma}, \boldsymbol{\zeta})]. \tag{S47}$$

This implies a fluctuation relation analogous to Eq. (S37),

$$\big\langle \exp(\Theta_p + \Theta_h + \Delta\Sigma) \big\rangle_{t_0, t_f} = 1, \tag{S48}$$

where $\Sigma(\Gamma, \zeta) = -\log Q(\Gamma, \zeta)$ is the local entropy of the joint state distribution. The partial fluxes of pathogen and host are related to conditional probabilities,

$$\frac{G(\mathbf{\Gamma}|\boldsymbol{\zeta})}{G(\mathbf{\Gamma}^T|\boldsymbol{\zeta}^T)} \quad = \quad \exp[\Theta_p(\mathbf{\Gamma}, \boldsymbol{\zeta})], \tag{S49}$$

$$\frac{G(\boldsymbol{\zeta}|\mathbf{\Gamma})}{G(\boldsymbol{\zeta}^T|\mathbf{\Gamma}^T)} \quad = \quad \exp[\Theta_h(\mathbf{\Gamma}, \boldsymbol{\zeta})], \tag{S50}$$

leading to fluctuation relations

$$\big\langle \exp(\Theta_p + \Delta\Sigma_p) \big\rangle_{t_0, t_f}(\boldsymbol{\zeta}) \quad = \quad 1, \tag{S51}$$

$$\big\langle \exp(\Theta_h + \Delta\Sigma_h) \big\rangle_{t_0, t_f}(\mathbf{\Gamma}) \quad = \quad 1. \tag{S52}$$

The corresponding deterministic relations

$$\Theta_p(\mathbf{\Gamma}, \boldsymbol{\zeta}) \quad \geq \quad 0, \tag{S53}$$

$$\Theta_h(\mathbf{\Gamma}, \boldsymbol{\zeta}) \quad \geq \quad 0, \tag{S54}$$

are used in the main text; see also Fig. 4C. The host flux relation (S54) distinguishes instantaneous-update control from computational protocols, which result from a nonlocal control dynamics and often have piecewise negative Θ_h (Fig. 4F,J).

Computational control. In this paper, we consider the class of scoring functions for computational control defined by Eq. (9),

$$\Omega(\mathbf{\Gamma}, \boldsymbol{\zeta}) = \int_{t_0}^{t_f} \psi_h(\Gamma(t'), \zeta(t')) \, dt' - \lambda T_\delta(\mathbf{\Gamma}, \boldsymbol{\zeta}), \tag{S55}$$

which is defined for paths $(\mathbf{\Gamma}, \boldsymbol{\zeta})$ extending over a control period $T \equiv t_f - t_0$. The first term on the r.h.s. is the integral of the instantaneous payoff function $\psi_h(\Gamma, \zeta)$ evaluated on the path $(\mathbf{\Gamma}, \boldsymbol{\zeta})$. The second term penalizes the total time the path $(\mathbf{\Gamma}, \boldsymbol{\zeta})$ remains below a payoff maximum ψ_h^* by more than a margin δ. By defining the modified payoff function

$$\psi_\lambda(\Gamma, \zeta) = \psi_h(\Gamma, \zeta) - \lambda H_\delta(\psi_h^* - \psi_h(\Gamma, \zeta)) \tag{S56}$$

with $H_\delta(x) = 1$ for $x > \delta$ and $H_\delta(x) = 0$ otherwise, we can write the scoring function as an integral,

$$\Omega(\mathbf{\Gamma}, \boldsymbol{\zeta}) = \int_{t_0}^{t_f} \psi_\lambda(\Gamma(t'), \zeta(t'))\, dt'. \tag{S57}$$

For the subsequent analysis, it is convenient to define the reduced score

$$\Delta\Omega(\mathbf{\Gamma}, \boldsymbol{\zeta}) = \int_{t_0}^{t_f} \Delta\psi_\lambda(\Gamma(t'), \zeta(t'))\, dt', \tag{S58}$$

where $\Delta\psi_\lambda(\Gamma, \zeta) = \psi_\lambda(\Gamma, \zeta) - C$ with an offset C that will be specified below.

For a given control protocol ζ, we define the expectation value of the scoring function (S58),

$$\begin{aligned} \langle \Delta\Omega \rangle(\boldsymbol{\zeta}) &= \Big\langle \int_{t_0}^{t_f} \Delta\psi_\lambda(\Gamma(t'), \zeta(t'))\, dt' \Big\rangle \\ &\equiv \int \Delta\Omega(\mathbf{\Gamma}, \boldsymbol{\zeta})\, \mathcal{P}(\mathbf{\Gamma}|\boldsymbol{\zeta})\, \mathcal{D}\mathbf{\Gamma}, \end{aligned} \tag{S59}$$

where $\mathcal{P}(\mathbf{\Gamma}|\boldsymbol{\zeta})$ denotes the conditional probability distribution over trait paths $\mathbf{\Gamma}$ generated by the stochastic process of pathogen evolution under the protocol ζ. Optimized computational protocols maximize this expectation value, a problem that can be solved by a transfer matrix approach. We consider the expected score (S59) for the set of paths defined in a partial time segment (t, t_f) $(t_0 \le t < t_f)$ and constrained to a pathogen initial state $\Gamma(t) = G$,

$$\langle \Delta\Omega \rangle(\boldsymbol{\zeta}; G, t) = \Big\langle \int_{t}^{t_f} \Delta\psi_\lambda(\Gamma(t'), \zeta(t'))\, dt' \Big\rangle_{\Gamma(t)=G}, \tag{S60}$$

and we define the conditional optimized protocol $\boldsymbol{\zeta}^*(G, t)$ and the corresponding payoff integral $J(G, t)$,

$$\boldsymbol{\zeta}^*(G, t) = \arg\max_{\boldsymbol{\zeta}} \Delta\Omega(\boldsymbol{\zeta}; G, t), \qquad J(G, t) = \max_{\boldsymbol{\zeta}} \Delta\Omega(\boldsymbol{\zeta}; G, t). \tag{S61}$$

For pathogen evolution by common mutations described in a diffusion approximation of the form (17), this conditional optimum can be shown to satisfy the local relation [15]

$$\frac{\partial}{\partial t} J(G, t) = \max_{\zeta} \left[\Delta\psi_\lambda(G, \zeta) - V_\Gamma(G, \zeta) \frac{\partial}{\partial G} J(G, t) - \frac{D}{2} \frac{\partial^2}{\partial G^2} J(G, t) \right], \tag{S62}$$

where $V_\Gamma(G, \zeta) = D\, \partial_G \psi_p(G, \zeta)$ is the deterministic pathogen velocity in Eq. (17). This relation is known as the Hamilton-Jacobi-Bellman equation for continuous-time stochastic control [15]. It can be used to compute the optimal solution $J(G, t)$ and the associated optimal control protocol $\boldsymbol{\zeta}^*(G, t)$ by recursion backwards in time. In the control theory literature, the path optimization problem is often formulated in terms of the cost function $(-\Omega(\mathbf{\Gamma}, \boldsymbol{\zeta}))$, and the conditional optimum $(-J(G, t))$ is referred to as the cost-to-go function.

Here we are interested in the deterministic control problem ($D = 0$) with boundary conditions

$$\Gamma(t) = G, \qquad \lim_{t \to \infty} \Gamma(t) = \Gamma^*; \tag{S63}$$

these control paths link a given initial pathogen state with the computational equilibrium point (Γ^*, ζ^*) given by Eq. (8). Choosing the offset $C = \psi_h^*$, the scoring function (S58) has a finite limit

$$\lim_{t_f \to \infty} \int_{t_0}^{t_f} \Delta\psi_\lambda((\Gamma(t'), \zeta(t'))\, dt' = \int_G^{\Gamma^*} \frac{\Delta\psi_\lambda(\Gamma, \zeta)}{V_\Gamma(\Gamma, \zeta)}\, d\Gamma. \tag{S64}$$

We can then solve Eq. (S62) along the maximum-core control path $(\boldsymbol{\Gamma}^*, \boldsymbol{\zeta}^*)$ by the method of characteristics. Because the payoff function has no explicit time dependence, the solution only depends on the initial trait value,

$$\begin{aligned} J(G) &= \int_{t_0}^{\infty} \Delta\psi_\lambda((\Gamma^*(t'), \zeta^*(t'))\, dt' && \text{(S65)} \\ &= \int_G^{\Gamma^*} \max_\zeta \frac{\Delta\psi_\lambda(\Gamma, \zeta)}{V_\Gamma(\Gamma, \zeta)}\, d\Gamma, && \text{(S66)} \end{aligned}$$

which is equivalent to the local path condition given in Eq.([22),

$$\zeta^*(\Gamma) = \arg\max_\zeta \frac{\Delta\psi_\lambda(\Gamma, \zeta)}{V_p(\Gamma, \zeta)}. \tag{S67}$$

In the main text, we use a extented HJB calculus to compute control paths compounded of common mutations treated in diffusion approximation and discrete, large-effect mutations. In the case of adaptive trait formation, Eq. (31]) an initial protocol with a gain-of-function mutation of effect G is prepended to a breeding protocol with starting point G and optimal score $J(G)$ given by Eq.)S66). Here, the duration of the initial step is part of the optimization of the combined protocol. Similarly, the protocol for metastable control, Eq. (37), consists of a baseline protocol with recurrent escape mutations of effect G compounded with a separable rescue protocol with optimal score $J(G)$. Here, the frequency of escape mutations is part of the optimization of the combined protocol.

Accessibility of the computational equilibrium. Here we analyze the evolutionary stability of the computational equilibrium protocol (Γ^*, ζ^*) under local dynamics of pathogen and host, as given by Eqs. (17) and (19). We use the deterministic form

$$\begin{pmatrix} \dot{\Gamma} \\ \dot{\zeta} \end{pmatrix} = \begin{pmatrix} V_\Gamma \\ V_\zeta \end{pmatrix} \tag{S68}$$

with the velocity field

$$\begin{pmatrix} V_\Gamma \\ V_\zeta \end{pmatrix} (\Gamma, \zeta) = \begin{pmatrix} \Delta_p\, \partial_\Gamma f_p \\ \Delta_h\, \partial_\zeta f_h \end{pmatrix} (\Gamma, \zeta). \tag{S69}$$

Both components of the deterministic dynamics (S68) take the form of Breeder's equation. Here we have omitted the entropic force contained in Eqs. (17) and [1], which is appropriate for large pathogen populations. In our model of ecological control, (G^*, λ^*) is a fixed point of the deterministic dynamics,

$$\begin{pmatrix} V_\Gamma \\ V_\zeta \end{pmatrix} (\Gamma^*, \zeta^*) = 0. \tag{S70}$$

Using Eqs. (12), the stability of this fixed point can be expressed in terms of the binding probability,

$$\begin{pmatrix} \partial_\Gamma V_\Gamma & \partial_\zeta V_\Gamma \\ \partial_\Gamma V_\zeta & \partial_\zeta V_\zeta \end{pmatrix} (\Gamma,\zeta) = \begin{pmatrix} -q_{ph}\Delta_p\, \partial_\Gamma^2 P_{\rm bind} & -q_{ph}\Delta_p\, \partial_\zeta \partial_\Gamma P_{\rm bind} \\ q_{ph}q_{hp}\Delta_h\, \partial_\Gamma \partial_\zeta P_{\rm bind} & q_{ph}q_{hp}\Delta_h\, \partial_\zeta^2 P_{\rm bind} \end{pmatrix} (\Gamma,\zeta) \tag{S71}$$

with $p_{\rm bind}(\Gamma,\zeta)$ given by Eq. (11). It is straightforward that this matrix is negative-definite in the parameter regime of interest; $c_p/q_{ph} < 1/4$. Hence, the computational equilibrium point (G^*,λ^*) is a stable fixed point of the deterministic evolutionary dynamics given by Eq. (S69). In contrast, in our model of evolutionary control, (G^*,λ^*) is not a fixed point of the deterministic host-pathogen dynamics. In this case, the velocity field (S69) has a component $V_\zeta(G^*,\lambda^*) \neq 0$, i.e., the host can gain a transient payoff advantage by moving away from the optimal stationary amplitude ζ^*. Hence, computational equilibrium point (G^*,λ^*) cannot be reached or maintained by a local control dynamics.

In Fig. S2, we compare computational and instantaneous-update control paths for ecological and evolutionary control. Consistent with the above stability analysis, deterministic local-update paths for ecological control converge to (G^*,λ^*); greedy-update control paths converge to the same point. The corresponding stochastic paths, which follow the dynamical equations (17) and (19) or (20), get localized to the neighborhood of (G^*,λ^*). For evolutionary control, however, these paths converge or get localized to a Nash equilibrium point $(\Gamma^\dagger,\zeta^\dagger)$ that has lower payoff than (G^*,λ^*).

Maximum-score paths always converge to the computational equilibrium point (G^*,λ^*) (Figs. 4D, S2). We note that these paths are obtained by backward iteration of the Hamilton-Jacobi-Bellman equation (S62) or, equivalently, by evaluation of the local condition (S67). We can compare these paths to path-optimized control with a different boundary condition, $\lim_{t\to\infty}\Gamma(t) = \hat\Gamma$, where $(\hat\Gamma,\hat\zeta) = \arg\max_{\Gamma,\zeta}\psi_h(\Gamma,\zeta)$ is the point of the absolute host payoff maximum. The deterministic control path converging to $(\hat\Gamma,\hat\zeta)$ is a well-defined solution of the Hamilton-Jacobi-Bellman equation with an asymptotic host payoff $f_h(\hat\Gamma,\hat\zeta) > f_h^*$; however, this solution has to be discarded on biological grounds. The fixed point $(\hat\Gamma,\hat\zeta)$ corresponds to a minimum of the pathogen fitness with respect to trait variation, $(\hat\Gamma,\hat\zeta) = \arg\min_\Gamma f_p(\Gamma,\hat\zeta)$ (the locus of these minima is shown as a dotted line in Fig. 2 and Fig. S2). Hence, the pathogen population is under disruptive selection, i.e., mutants with $G < \hat\Gamma$ and with $G > \hat\Gamma$ are under positive selection. These mutants cannot be simultaneously contained by control selection of the form $f_p \sim P_{\rm bind}$ considered in this paper. We conclude that stationary control has to be in an evolutionarily stable pathogen state, as described by the condition $(\Gamma^*,\zeta^*) = \arg\max_\Gamma f_p(\Gamma,\zeta^*)$ in Eq. (8). Computational control protocols converging to such states are obtained by maximizing the host payoff integral, Eq. (9), with appropriate boundary conditions.

References

[1] Nourmohammad A, Schiffels S, Lässig M (2013) Evolution of molecular phenotypes under stabilizing selection. *Journal of Statistical Mechanics: Theory and Experiment* 2013(01):P01012.

[2] Held T, Klemmer D, Lässig M (2019) Survival of the simplest in microbial evolution. *Nature Communications* 10(1):2472.

[3] Kimura M (1983) *The Neutral Theory of Molecular Evolution.* (Cambridge University Press).

[4] Kingman JFC (1982) On the genealogy of large populations. *Journal of Applied Probability* 19(A):27–43.

[5] Neher RA, Hallatschek O (2013) Genealogies of rapidly adapting populations. *Proceedings of the National Academy of Sciences of the United States of America* 110(2):437–442.

[6] Pollett P (2001) Diffusion approximations for ecological models. *Proceedings of the International Congress on Modelling and Simulation* 2:843–848.

[7] Cremer J, Melbinger A, Frey E (2011) Evolutionary and population dynamics: A coupled approach. *Physical Review E - Statistical, Nonlinear, and Soft Matter Physics* 84(5):051921.

[8] Ovaskainen O, Meerson B (2010) Stochastic models of population extinction. *Trends in Ecology and Evolution* pp. 643–652.

[9] Jarzynski C (1997) Nonequilibrium equality for free energy differences. *Physical Review Letters* pp. 2690–2693.

[10] Crooks GE (1999) Entropy production fluctuation theorem and the nonequilibrium work relation for free energy differences. *Physical Review E - Statistical Physics, Plasmas, Fluids, and Related Interdisciplinary Topics* pp. 2721–2726.

[11] Seifert U (2005) Entropy production along a stochastic trajectory and an integral fluctuation theorem. *Physical Review Letters* p. 040602.

[12] Chertkov M, Jarzynski C, Chernyak VY (2006) Path-integral analysis of fluctuation theorems for general Langevin processes. *Journal of Statistical Mechanics: Theory and Experiment* pp. P08001–P08001.

[13] Seifert U (2012) Stochastic thermodynamics, fluctuation theorems and molecular machines. *Reports on Progress in Physics* p. 126001.

[14] Mustonen V, Lässig M (2010) Fitness flux and ubiquity of adaptive evolution. *Proceedings of the National Academy of Sciences* 107(9):4248–4253.

[15] Kappen HJ (2007) An introduction to stochastic control theory, path integrals and reinforcement learning in *AIP Conference Proceedings*. pp. 149–181.

Supporting Figures

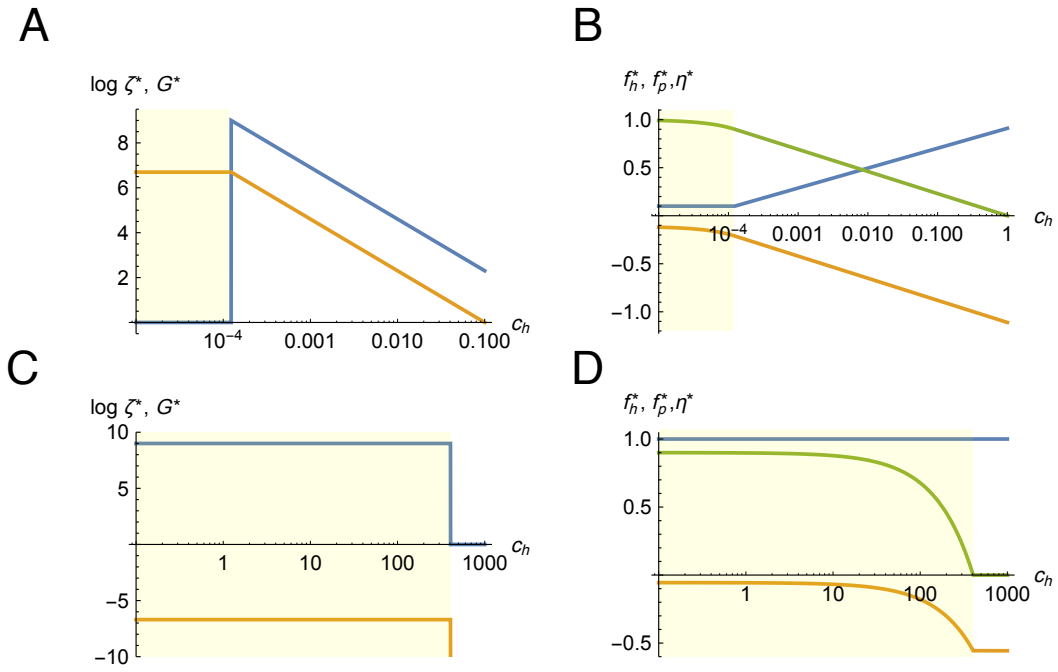

Figure S1: Computational equilibrium protocols. (A, B) Ecological control, (C, D) evolutionary control. (A, C) Equilibrium log control amplitude, $\log \zeta^*$ (orange), and pathogen trait, G^* (blue), as functions of the control cost, c_h. Yellow shading marks the strong control regime. (B, D) Host payoff, f_h^* (orange), pathogen fitness, f_p^* (blue), and control efficiency, η^* (green), as functions of c_h. Model parameters: $f_p = 1, q_{ph} = 1/q_{ph} = 0.9, c_p = 0.09$ (ecological control); $f_{p,0} = 1, q_{ph} = 0.9, q_{hp} = 5/9, c_p = 0.09, c_h = 5$ (evolutionary control).

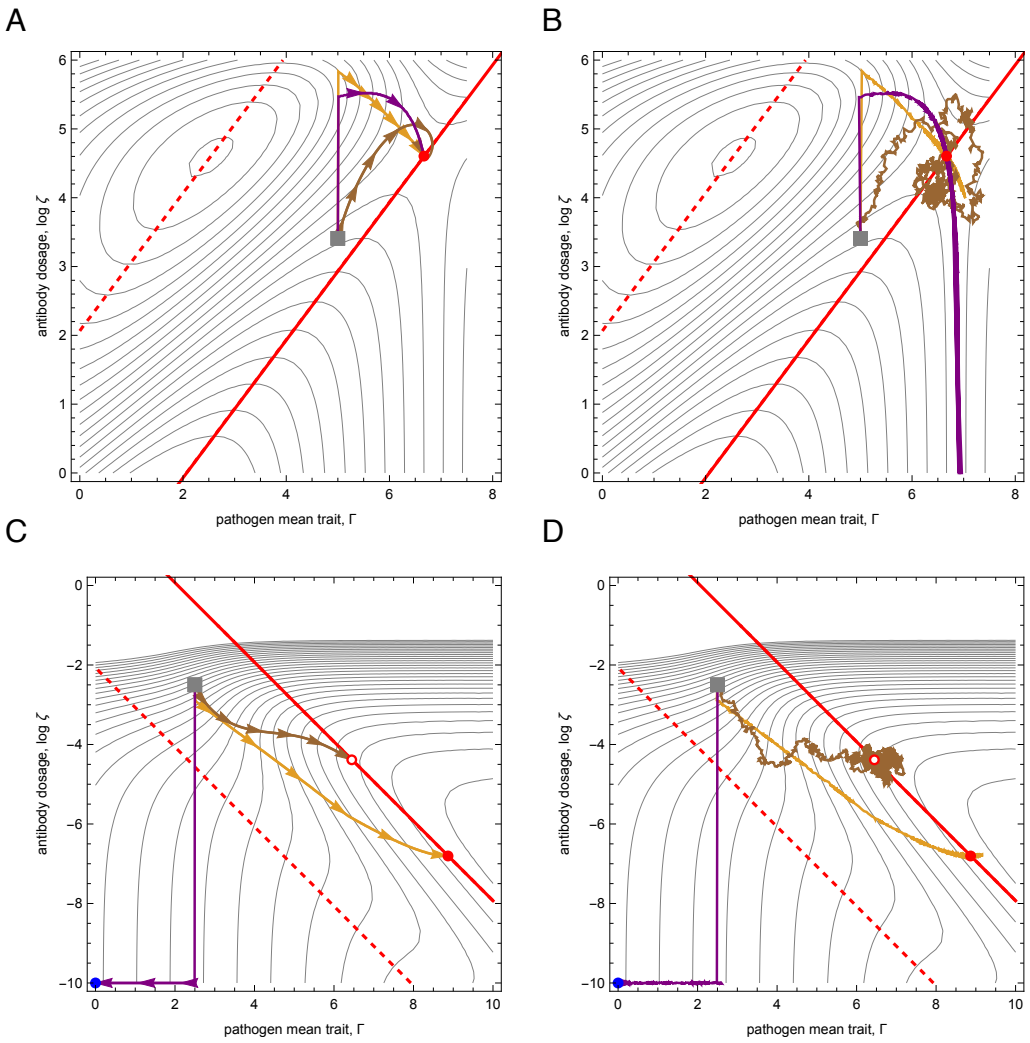

Figure S2: Dynamical accessibility of the computational equilibrium point. The figure compares maximum-score computational control paths (orange) with local (brown) and greedy (purple) instantaneous-update paths (left panels: deterministic, right panels: stochastic). These paths start from a common initial condition (grey square). Deterministic paths converge to, stochastic paths get localized around, the computational equilibrium point (Γ^*, ζ^*) given by Eq. [10] (red dot), the Nash equilibrium point $(\Gamma^\dagger, \zeta^\dagger)$ given by Eq. [9] (red open circle), or the no-control fixed point (blue). Host payoff is marked by contours; cf. Fig. 2B. (A) Ecological control. All paths converge/get localized to the computational equilibrium point, which is also a Nash equilibrium. (B) Evolutionary control. The computational control path converges to (Γ^*, ζ^*), but this point cannot be reached by instantaneous-update dynamics. Local-update and greedy paths converge/get localized to the Nash equilibrium $(\Gamma^\dagger, \zeta^\dagger)$, or to no control fixed point, both have lower host payoff than the computational equilibrium. Parameters are as in Fig. 4.

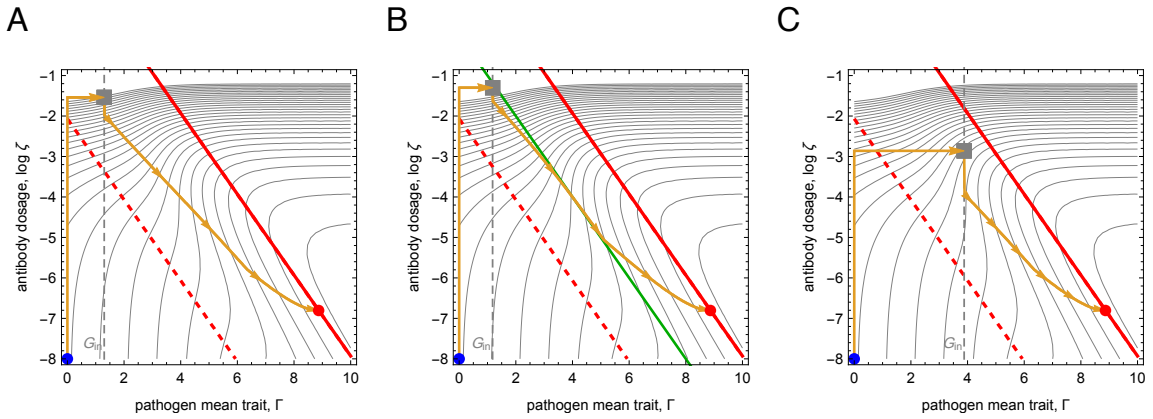

Figure S3: Computational control dynamics depends on sequence diversity and speed parameter. The maximum-score control path is shown for different values of the trait sequence diversity and the speed parameter: (A) $\theta = 1, \lambda = 0$ (as in Fig. 4D), (B) $\theta = 1, \lambda = 1$, (C) $\theta = 50, \lambda = 0$. Weighing in the speed of control ($\lambda = 1$) moves the control path closer to the path of maximal adaptive speed V_Γ (green line). This path is given by $\log \zeta(\Gamma) = -\Gamma$; i.e., the antibody dosage equals the Γ-dependent dissociation constant. Other model parameters as in Fig. 4.

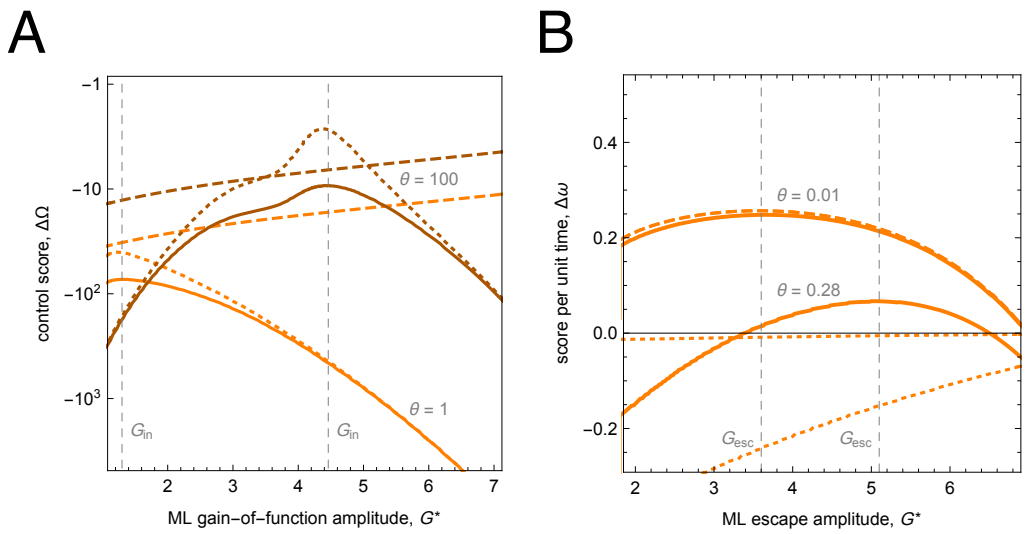

Figure S4: Tuning fitness valleys by computational control. The figure illustrates the extented HJB calculus, Eq. (31) and (37), used to optimize control paths across pathogen fitness valleys. (A) Adaptive trait formation. The initial-phase score, $\Delta\Omega_{\rm in}$ (dashed), the optimal breeding score, $J_{\rm br}$ (dotted), and the total score, $\Delta\Omega = \Delta\Omega_{\rm in} + J_{\rm br}$ (solid) are plotted against the maximum-likelihood gain-of-function trait $G^\star(\zeta)$ for $\theta = 1, 10^2$ and initiation amplitude $\log\zeta$ varying in the range $[1, 6]$ (darker lines indicate protocols with clonal interference in the breeding phase). All scores measure time-integrated differences of the adaptive protocol compared to the computational equilibrium. The score maximum determines the optimal compound protocol $(G_{\rm in}, \zeta_{\rm in})$; see Eqs. (31 – 36). This protocol circumvents the pathogen fitness valley preventing gain of function in the uncontrolled state: a high initiation dosage $\zeta_{\rm in}$ sets an amplitude $G_{\rm in} = G^*(\zeta_{\rm in})$ where gain-of-function mutations are more frequent. (B) Metastable control. The baseline score, $\Delta\omega_{\rm base}$ (dashed), the rescue score, $vJ_{\rm res}$ (dotted), and the total score, $\Delta\omega = \omega_{\rm base} + v\Delta J_{\rm res}$ (solid) are plotted against the maximum-likelihood gain-of-function trait $G^\star(\zeta)$ for $\theta = 10^{-2}$ and 0.28 (close to θ_c) and baseline amplitude $\log\zeta$ varying in the range $[1, 6.5]$. All scores measure time-averaged differences of the metastable protocol compared to the computational equilibrium (red line). The score maximum determines the optimal compound protocol $(G_{\rm esc}, \zeta_{\rm base})$; see Eqs. (37 – 41). This protocol broadens the pathogen fitness valley for resistance evolution compared to optimal control of the wild type, $(\Gamma_{\rm wt} = 0, \zeta_0 = \arg\max_\zeta \psi_h(0,\zeta))$: an enhanced baseline dosage $\zeta_{\rm base} > \zeta_0$ sets an amplitude $G_{\rm esc}(\zeta_{\rm base})$ where escape mutations are rarer. Model parameters: $N_e = 10^6$, $x_{\rm esc} = 0.05$, $a = 2$, other parameters as in Fig. 4.